GEOPHYSICS, VOL. 72, NO. 6 (NOVEMBER-DECEMBER 2007); P. D119–D127, 4 FIGS., 4 TABLES.
10.1190/1.2768402

Ray velocity and ray attenuation in homogeneous anisotropic viscoelastic media

Václav Vavryčuk[1]

ABSTRACT

Asymptotic wave quantities such as ray velocity and ray attenuation are calculated in anisotropic viscoelastic media by using a stationary slowness vector. This vector generally is complex valued and inhomogeneous, and it predicts the complex energy velocity parallel to a ray. To compute the stationary slowness vector, one must find two independent, real-valued unit vectors that specify the directions of its real and imaginary parts. The slowness-vector inhomogeneity affects asymptotic wave quantities and complicates their computation. The critical quantities are attenuation and quality factor (Q-factor); these can vary significantly with the slowness-vector inhomogeneity. If the inhomogeneity is neglected, the attenuation and the Q-factor can be distorted distinctly by errors commensurate to the strength of the velocity anisotropy — as much as tens of percent for sedimentary rocks. The distortion applies to strongly as well as to weakly attenuative media. On the contrary, the ray velocity, which defines the wavefronts and physically corresponds to the energy velocity of a high-frequency signal propagating along a ray, is almost insensitive to the slowness-vector inhomogeneity. Hence, wavefronts can be calculated in a simplified way except for media with extremely strong anisotropy and attenuation.

INTRODUCTION

Most rocks are to some extent anisotropic and attenuative. Anisotropy mainly affects a directionally dependent propagation velocity of seismic waves, whereas attenuation controls directionally dependent dissipation of seismic energy and, consequently, a decay of wave amplitudes along a raypath. A simple model reflecting both wave phenomena is an anisotropic viscoelastic medium described by complex-valued, frequency-dependent, viscoelastic parameters (Auld, 1973; Carcione, 2001). This model has been applied mainly to propagation of plane waves (Carcione and Cavallini, 1993; Deschamps et al., 1997; Shuvalov and Scott, 1999; Deschamps and Assouline, 2000; Červený and Pšenčík, 2005, 2006; Zhu and Tsvankin, 2006, 2007), whereas the modeling of wavefields generated by point sources is less developed (Carcione, 1994; Carcione et al., 1996; Audoin and Guilbaud, 1998). Complete wavefields usually are computed by using time-demanding numerical methods that directly solve the wave equation (Carcione et al., 1988; Carcione, 1990; Saenger and Bohlen, 2004; Moczo et al., 2007). On the other hand, asymptotic wavefields are calculated more efficiently but existing formulas are valid only for weakly anisotropic, weakly attenuating media.

This article deals with the high-frequency properties of wavefields generated by point sources and propagating in anisotropic viscoelastic media of arbitrary strength of anisotropy and attenuation. Through application of the steepest-descent method to an exact solution, I derive asymptotic wave quantities such as ray velocity, ray attenuation, and ray quality factor. I discuss their physical meaning and show how to calculate them. Finally, by using numerical examples, I demonstrate how their values can be distorted when applying a simplified, commonly used approach (Carcione, 1994; Carcione et al., 2003; Zhu and Tsvankin, 2006, 2007).

In formulas, real and imaginary parts of complex-valued quantities are denoted by superscripts R and I, respectively. A complex-conjugate quantity is denoted by an asterisk. The direction of a complex-valued vector $\mathbf{v}$ is calculated as $\mathbf{v}/\sqrt{\mathbf{v}\cdot\mathbf{v}}$, where the dot means the scalar product (the normalization condition $\mathbf{v}/\sqrt{\mathbf{v}\cdot\mathbf{v}^*}$ is not used because it complicates generalizing some of the real equations to complex ones). The magnitude of complex-valued vector $\mathbf{v}$ is $\sqrt{\mathbf{v}\cdot\mathbf{v}}$. If any complex-valued vector is defined by a real-valued direction, the vector is called homogeneous. If defined by a complex-valued direction, the vector is called inhomogeneous. In formulas, the Einstein summation convention is used for repeated subscripts.

PLANE WAVES IN AN ANISOTROPIC VISCOELASTIC MEDIUM

Let us assume a time-harmonic plane wave described by the displacement

$$u_i(\mathbf{x},t) = U(\mathbf{x})g_i \exp[-i\omega(t - \mathbf{p}\cdot\mathbf{x})], \qquad (1)$$

Manuscript received by the Editor 4 March 2007; revised manuscript received 21 May 2007; published online 5 September 2007.
[1]Academy of Sciences, Institute of Geophysics, Czech Republic. E-mail: vv@ig.cas.cz.

where $\mathbf{x}$ is the position vector, U is the amplitude, $\mathbf{g}$ is the unit polarization vector, ω is the circular frequency, and t is time. Vector $\mathbf{p}$ is the slowness vector defined as $\mathbf{p} = \mathbf{n}/c$, where $\mathbf{n}$ is the slowness direction and c is the phase velocity. Except for $\mathbf{x}$, ω, and t, all quantities are, in general, complex valued.

Velocity, attenuation, and inhomogeneity of plane waves

Because slowness vector $\mathbf{p}$ in equation 1 is complex valued, it describes not only the propagation velocity of plane waves but also their attenuation and inhomogeneity. Decomposing $\mathbf{p}$ yields

$$\mathbf{p} = \lfloor (V^{\text{phase}})^{-1} + iA^{\text{phase}} \rfloor \mathbf{s} + iD^{\text{phase}}\mathbf{t}, \tag{2}$$

where V^{phase}, A^{phase}, and D^{phase} are real-valued scalars called the phase velocity, phase attenuation, and phase inhomogeneity. Vectors $\mathbf{s}$ and $\mathbf{t}$ are real-valued, mutually perpendicular unit vectors, $\mathbf{s}$ is normal to the wavefront, and $\mathbf{t}$ lies in the wavefront. Furthermore, we define real-valued vectors:

$$\mathbf{V}^{\text{phase}} = V^{\text{phase}}\mathbf{s}, \quad \mathbf{A}^{\text{phase}} = A^{\text{phase}}\mathbf{s}, \quad \mathbf{D}^{\text{phase}} = D^{\text{phase}}\mathbf{t}, \tag{3}$$

called the phase-velocity, phase-attenuation, and phase-inhomogeneity vectors. These quantities are observed and measured in experiments with plane waves and describe the propagation velocity of the wavefront, the exponential decrease of the amplitude along the normal to the wavefront, and the exponential decrease of the amplitude along the wavefront.

The decomposition performed in equation 2 differs from that commonly used. Usually, the slowness vector is decomposed just into its real and imaginary parts, called the propagation and attenuation vectors (see Aki and Richards, 2002, their equation 5.96; Červený and Pšenčík, 2005, their equation 6). The advantage of decomposition in equation 2 is that it further distinguishes between the medium attenuation and wave inhomogeneity.

Viscoelastic parameters and the Christoffel tensor

The propagation of plane waves is controlled by the tensor of complex-valued, density-normalized viscoelastic parameters $a_{ijkl} = c_{ijkl}/\rho$. The real and imaginary parts of a_{ijkl} describe elastic and viscous properties of the medium, and their ratio, called the matrix of quality factors,

$$q_{ijkl} = -\frac{a^{\text{R}}_{ijkl}}{a^{\text{I}}_{ijkl}}, \tag{4}$$

quantifies how attenuative the medium is (there is no summation over repeated indices). Attenuation can also be described by a scalar quantity Q called the quality factor or the Q-factor (Carcione, 2000, his equation 14; Chichinina et al., 2006, their equation 27):

$$Q^{\text{phase}} = -\frac{(c^2)^{\text{R}}}{(c^2)^{\text{I}}}. \tag{5}$$

The superscript "phase" highlights that Q is calculated from the complex-valued phase velocity c and thus primarily describes attenuation of plane waves. Obviously, the quality factor is, in general, directionally dependent in anisotropic media. Note that equations 4 and 5, which define the quality matrix and quality factor, respectively, depend on the form of the time-harmonic wave specified in equation 1. For waves with exponential factor $\exp[i\omega(t - \mathbf{p}\cdot\mathbf{x})]$, the definitions must be modified by omitting the minus sign in equations 4 and 5.

Parameters a_{ijkl} are used for constructing Christoffel tensor Γ_{jk}, which is defined either in terms of the slowness direction $\mathbf{n}$,

$$\Gamma_{jk}(\mathbf{n}) = a_{ijkl}n_i n_l, \tag{6}$$

or in terms of the slowness vector $\mathbf{p}$,

$$\Gamma_{jk}(\mathbf{p}) = a_{ijkl}p_i p_l. \tag{7}$$

The slowness direction $\mathbf{n}$ is real valued for homogeneous waves but complex valued for inhomogeneous waves. The Christoffel tensor Γ_{jk} has three eigenvalues and three eigenvectors, calculated by using the Christoffel equation:

$$(\Gamma_{jk} - G\delta_{jk})g_j = 0. \tag{8}$$

The eigenvalues $G(\mathbf{n})$ and $G(\mathbf{p})$ read

$$G(\mathbf{n}) = a_{ijkl}n_i n_l g_j g_k = c^2 \tag{9}$$

and

$$G(\mathbf{p}) = a_{ijkl}p_i p_l g_j g_k = 1, \tag{10}$$

defining phase velocity c and slowness vector $\mathbf{p}$ as a function of slowness direction $\mathbf{n}$. The eigenvectors define polarization vectors $\mathbf{g}$. The polarization vectors are normalized, so that $\mathbf{g}\cdot\mathbf{g} = 1$.

From the eigenvalue $G(\mathbf{p})$, we further derive the complex energy velocity as

$$v_i = \frac{1}{2}\frac{\partial G}{\partial p_i} = a_{ijkl}p_l g_j g_k, \tag{11}$$

which is called the group velocity in elastic media. Vectors $\mathbf{v}$ and $\mathbf{p}$ are related by the equation

$$\mathbf{v}\cdot\mathbf{p} = 1. \tag{12}$$

WAVES GENERATED BY POINT SOURCES

Exact solution

The exact Green's function in unbounded, homogeneous, anisotropic viscoelastic media can be expressed in the frequency domain as the sum of regular and singular terms, $G^{\text{reg}}_{kl}(\mathbf{x},\omega)$ and $G^{\text{sing}}_{kl}(\mathbf{x},\omega)$, as follows (see Vavryčuk, 2007, his equations 3.1–3.3):

$$G_{kl}(\mathbf{x},\omega) = G^{\text{reg}}_{kl}(\mathbf{x},\omega) + G^{\text{sing}}_{kl}(\mathbf{x}), \tag{13}$$

$$G_{kl}^{\mathrm{reg}}(\mathbf{x},\omega) = \frac{i\omega}{8\pi^2\rho}\sum_{M=1}^{3}\int\limits_{\substack{S(\mathbf{n})\\ \mathbf{n}\cdot\mathbf{x}>0}}\frac{g_k^{(M)}g_l^{(M)}}{(c^{(M)})^3} \times\exp\left(i\omega\frac{\mathbf{n}\cdot\mathbf{x}}{c^{(M)}}\right)dS(\mathbf{n}), \quad (14)$$

$$G_{kl}^{\mathrm{sing}}(\mathbf{x},\omega) = \frac{1}{8\pi^2\rho}\sum_{M=1}^{3}\int\limits_{S(\mathbf{n})}\frac{g_k^{(M)}g_l^{(M)}}{(c^{(M)})^2}\delta(\mathbf{n}\cdot\mathbf{x})dS(\mathbf{n}). \quad (15)$$

Superscript $M=1,2,3$ denotes the type of wave (P, S1, or S2), $\mathbf{g}$ is the unit polarization vector, c is the phase velocity, ρ is the density of the medium, $\mathbf{x} = \mathbf{N}r$ is the position vector, r is the distance of the observation point from the source, $\mathbf{N}$ is the ray vector, $\mathbf{n}$ is the unit wave normal, and $S(\mathbf{n})$ is the unit sphere. The regular term is integrated over a hemisphere, defined by $\mathbf{n}\cdot\mathbf{x} > 0$. The singular term is integrated formally over a whole sphere, but the Dirac delta function $\delta(\mathbf{n}\cdot\mathbf{x})$ in the integrand reduces the surface integral to a line integral, hence the singular term is integrated over a unit circle defined by $\mathbf{n}\cdot\mathbf{x} = 0$. Phase velocity c, slowness vector $\mathbf{p}$, complex energy velocity v, and polarization vector $\mathbf{g}$ are, in general, complex valued and frequency dependent. Wave normal $\mathbf{n}$, ray vector $\mathbf{N}$, position vector $\mathbf{x}$, and density ρ are real valued and do not depend on real-valued frequency ω.

The integration in equations 14 and 15 also can be performed over slowness surface $S(\mathbf{p})$. After transforming the surface element $dS(\mathbf{n})$ to $dS(\mathbf{p})$ (see Burridge, 1967), we can write for a particular P-, S1-, or S2-wave (see Vavryčuk, 2007, his equations 3.6 and 3.7),

$$G_{kl}^{\mathrm{reg}}(\mathbf{x},\omega) = \frac{i\omega}{8\pi^2\rho}\int\limits_{\substack{S(\mathbf{p})\\ \mathbf{n}\cdot\mathbf{x}>0}}\frac{g_k g_l}{v}\exp(i\omega\mathbf{p}\cdot\mathbf{x})dS(\mathbf{p}), \quad (16)$$

$$G_{kl}^{\mathrm{sing}}(\mathbf{x},\omega) = \frac{1}{8\pi^2\rho}\int\limits_{S(\mathbf{p})}\frac{g_k g_l}{v}\delta(\mathbf{p}\cdot\mathbf{x})dS(\mathbf{p}). \quad (17)$$

The complete Green's function is then a sum of contributions for all three waves. When $\omega = 0$, the regular term G_{kl}^{reg} vanishes and the singular term G_{kl}^{sing} becomes the static Green's function.

Asymptotic solution

Let us assume high-frequency ω and an observation point far from the source (at about 10 wavelengths or more; see Vavryčuk, 2007). Then, singular term G_{kl}^{sing} (equation 17) becomes negligible and regular term G_{kl}^{reg} (equation 16) can be evaluated asymptotically. By applying the steepest-descent method (Ben-Menahem and Singh, 1981, their Appendix E) to the integral in equation 16, we obtain the asymptotic Green's function G_{kl}^{asym} in the following form (see Vavryčuk, 2007, his equation 4.11):

$$G_{kl}^{\mathrm{asym}}(\mathbf{x},\omega) = \frac{1}{4\pi\rho}\frac{g_k g_l}{v\sqrt{|K|}}\frac{1}{r}\exp(i\sigma_0 + i\omega\mathbf{p}_0\cdot\mathbf{x}), \quad (18)$$

where

$$\sigma_0 = -\frac{1}{2}(\varphi_1 + \varphi_2),$$
$$-\frac{3}{2}\pi \le \varphi_1 < \frac{1}{2}\pi,$$
$$-\frac{3}{2}\pi \le \varphi_2 < \frac{1}{2}\pi,$$

and $\mathbf{p}_0$ is the stationary slowness vector, defined as the vector predicting the complex energy velocity (equation 11) to be homogeneous and parallel to a ray.

Equation 18 generalizes the result obtained for elastic media (Burridge, 1967; Yeatts, 1984; Every and Kim, 1994) and holds for all shapes of the slowness surface and for all ray directions except for the vicinity of singularities on a slowness surface (see Vavryčuk, 1999, 2002) and cusp edges on a wavefront, where more involved approaches are required. The complications arise because of a rapid change of polarization vectors near a singularity and because of close positions of stationary slowness vectors near a cusp edge.

Quantity $K = K_1K_2$ is the Gaussian curvature of the slowness surface, K_1 and K_2 are the principal curvatures, and φ_1 and φ_2 are their phase angles. All quantities dependent on $\mathbf{p}$ in equation 18 are taken at stationary slowness vector $\mathbf{p}_0$. Position vector $\mathbf{x} = r\mathbf{N}$, distance r, ray vector $\mathbf{N}$, frequency ω, phase angles φ_1 and φ_2, and density ρ are real valued, but polarization vector $\mathbf{g}$, Gaussian curvature K, principal curvatures K_1 and K_2, energy velocity v, and slowness vector $\mathbf{p}_0$ are complex valued.

The Green's function in equation 18 can be used for calculating high-frequency wavefields generated by simple forces. If the wavefield is generated by dipoles (see Aki and Richards, 2002, their equation 3.23) a high-frequency approximation of the spatial derivative of the Green's function is required:

$$\frac{\partial}{x_m}[G_{kl}^{\mathrm{asym}}(\mathbf{x},\omega)] = i\omega p_{0m}G_{kl}^{\mathrm{asym}}(\mathbf{x},\omega) = \frac{i\omega}{4\pi\rho}\frac{g_k g_l p_{0m}}{v\sqrt{|K|}}\frac{1}{r}\exp(i\sigma_0 + i\omega\mathbf{p}_0\cdot\mathbf{x}). \quad (19)$$

Ray velocity, attenuation, and quality factor

After decomposing the complex energy velocity v into real and imaginary parts, v^{R} and v^{I}, the exponential term in equation 18 reads

$$\exp(i\omega\mathbf{p}_0\cdot\mathbf{x}) = \exp\left(i\omega\frac{r}{v}\right) = \exp(-\omega A^{\mathrm{ray}}r)\exp\left(i\omega\frac{r}{V^{\mathrm{ray}}}\right), \quad (20)$$

where

$$V^{\mathrm{ray}} = \frac{vv^*}{v^{\mathrm{R}}} = \frac{v^{\mathrm{R}}v^{\mathrm{R}} + v^{\mathrm{I}}v^{\mathrm{I}}}{v^{\mathrm{R}}} \quad (21)$$

and

$$A^{\text{ray}} = -\frac{v^{\text{I}}}{vv^*} = -\frac{v^{\text{I}}}{v^{\text{R}}v^{\text{R}} + v^{\text{I}}v^{\text{I}}}. \quad (22)$$

Because V^{ray} and A^{ray} control the propagation velocity and the amplitude decay along a ray in equation 20, they are called the ray velocity and ray attenuation, respectively. They are real valued, and they can be observed and measured in wavefields generated by point sources.

Real-valued ray vector $\mathbf{N}$ and scalars V^{ray} and A^{ray} can be used to define real-valued vectors

$$\mathbf{V}^{\text{ray}} = V^{\text{ray}}\mathbf{N} \quad (23)$$

and

$$\mathbf{A}^{\text{ray}} = A^{\text{ray}}\mathbf{N},$$

called the ray-velocity and ray-attenuation vectors.

To complete the definitions of the ray quantities, the ray quality factor Q^{ray} is introduced as

$$Q^{\text{ray}} = -\frac{(v^2)^{\text{R}}}{(v^2)^{\text{I}}}, \quad (24)$$

where v is the complex energy velocity (equation 11) evaluated at stationary slowness vector $\mathbf{p}_0$.

The ray velocity V^{ray}, ray attenuation A^{ray}, and ray quality factor Q^{ray} have a physical meaning similar to that of the phase velocity V^{ray}, phase attenuation A^{phase}, and phase quality factor Q^{phase}. The only difference is that the ray quantities are defined along a ray, whereas the phase quantities are defined along a wave normal.

CALCULATING THE STATIONARY SLOWNESS VECTOR

Determining the stationary slowness vector $\mathbf{p}_0$ is the crucial and most complicated step in calculating asymptotic wave quantities in anisotropic viscoelastic media. The stationary slowness vector $\mathbf{p}_0$ can be determined either by iterations or by solving a system of polynomial equations.

The iterative procedure is fast and works well, provided that a wavefront is free of triplications. The procedure is based on seeking a complex-valued slowness direction $\mathbf{n}$ for which the complex energy velocity $\mathbf{v}$ is homogeneous and directed along a specified ray vector $\mathbf{N}$. This procedure needs an inversion of the following forward scheme. First, we use equation 6 to calculate Christoffel tensor $\Gamma_{jk}(\mathbf{n})$ for a specified complex-valued slowness direction $\mathbf{n}$. Second, we compute its eigenvalues and eigenvectors and construct the complex-valued slowness vector $\mathbf{p}$. Third, we calculate the complex energy velocity $\mathbf{v}$ using equation 11. Normalizing vector $\mathbf{v}$, we obtain ray vector $\mathbf{N}$.

When inverting this scheme, we fix a real-valued ray vector $\mathbf{N}$ and seek four unknown angles: two angles that define the real part and two others that define the imaginary part of slowness direction $\mathbf{n}_0$. The misfit function can be defined as the modulus of the complex-valued deviation between the fixed and predicted ray vectors. The inversion is nonlinear and can be performed by using standard methods (Press et al., 2002). After finding vector $\mathbf{n}_0$, the stationary slowness vector $\mathbf{p}_0$ is obtained readily by using equation 9 or 10.

If the wavefront is folded, the determination of stationary slowness $\mathbf{p}_0$ is more involved. When using iterations, we must be careful to find all slowness vectors corresponding to a given ray, a process that might be tricky sometimes. The other possibility is to follow Vavryčuk (2006) and solve a system of polynomial equations in unknown components of $\mathbf{p}_0$. The stationary slowness vector $\mathbf{p}_0$ is calculated from the real-valued ray vector $\mathbf{N}$ by solving the following equations:

$$D_{kk}N_i - a_{ijkl}D_{jk}p_{0l}p_{0m}N_m = 0, \quad (25)$$

where $i = 1,2,3$; D_{jk} is the matrix of cofactors of $\hat{D}_{jk} = \Gamma_{jk} - G\delta_{jk}$; and

$$\begin{aligned}
D_{11} &= (\Gamma_{22} - G)(\Gamma_{33} - G) - \Gamma_{23}^2,\\
D_{22} &= (\Gamma_{11} - G)(\Gamma_{33} - G) - \Gamma_{13}^2,\\
D_{33} &= (\Gamma_{11} - G)(\Gamma_{22} - G) - \Gamma_{12}^2,\\
D_{12} &= D_{21} = \Gamma_{13}\Gamma_{23} - \Gamma_{12}(\Gamma_{33} - G),\\
D_{13} &= D_{31} = \Gamma_{12}\Gamma_{23} - \Gamma_{13}(\Gamma_{22} - G),\\
D_{23} &= D_{32} = \Gamma_{12}\Gamma_{13} - \Gamma_{23}(\Gamma_{11} - G), \quad (26)
\end{aligned}$$

where $\Gamma_{jk} = \Gamma_{jk}(\mathbf{p}_0), G = G(\mathbf{p}_0) = 1$.

Equation 25 is a system of coupled polynomial equations of the sixth order in unknowns $\mathbf{p}_{01}$, $\mathbf{p}_{02}$, and $\mathbf{p}_{03}$. After solving the equations, we obtain a complete set of slowness vectors corresponding to all wave types and to all branches of the folded wave surface. The equations have been originally derived for elastic media, but they can be applied equally to viscoelastic media by considering parameters a_{ijkl} to be complex valued. Consequently, the retrieved slowness vector $\mathbf{p}_0$ becomes also complex valued.

Note that equation 25 also yields some spurious solutions that must be rejected by checking whether the complex energy velocity $\mathbf{v}$ (equation 11) is really homogeneous for a given slowness-vector solution. For details, see Vavryčuk (2006).

PHYSICAL MEANING OF RAY VELOCITY

The ray velocity V^{ray} is closely related to the so-called time-averaged energy velocity $\bar{V}^{\text{energy}}$ (Carcione and Cavallini, 1993; Carcione, 2001), defined as the velocity of time-averaged energy transmitted by a time-harmonic plane wave and expressed as (Červený and Pšenčík, 2006, equation 35)

$$\bar{V}_i^{\text{energy}} = \frac{S_i}{E} = \frac{(a_{ijkl}U_kU_j^*p_l)^{\text{R}}}{(a_{ijkl}U_kU_j^*p_l)^{\text{R}}p_i^{\text{R}}}. \quad (27)$$

Vector $\mathbf{S}$ is the real part of the time-averaged energy-flux vector, and E is the real-valued time-averaged total energy density of the propagating wave. Taking into account equation 11, we obtain

$$\bar{V}_i^{\text{energy}} = \frac{\bar{v}_i^{\text{R}}}{\bar{v}_k^{\text{R}}p_k^{\text{R}}}, \quad (28)$$

where $\bar{\mathbf{v}}$ means the time-averaged complex energy velocity.

For stationary $\mathbf{p}$, velocity $\bar{\mathbf{V}}^{\text{energy}}$ can be simplified further . Because $\mathbf{v} = \mathbf{N}v$ is a homogeneous vector having direction $\mathbf{N}$ independent of time, the time-averaged velocity vector $\bar{\mathbf{v}}^{\text{R}}$ can be substituted for by the instantaneous velocity vector $\mathbf{v}^{\text{R}} = \mathbf{N}v^{\text{R}}$:

$$\bar{V}_i^{\text{energy}} = \frac{v_i^{\text{R}}}{v_k^{\text{R}}p_k^{\text{R}}} = \frac{N_i}{N_kp_k^{\text{R}}}. \quad (29)$$

Taking into account that

$$v_i p_i = 1, \tag{30}$$

which is equivalent to

$$v_i^{\mathrm{R}} p_i^{\mathrm{R}} - v_i^{\mathrm{I}} p_i^{\mathrm{I}} = 1 \quad \text{and} \quad v_i^{\mathrm{R}} p_i^{\mathrm{I}} + v_i^{\mathrm{I}} p_i^{\mathrm{R}} = 0, \tag{31}$$

we can write

$$v^{\mathrm{R}} = (v^{\mathrm{R}} v^{\mathrm{R}} + v^{\mathrm{I}} v^{\mathrm{I}}) N_k p_k^{\mathrm{R}}. \tag{32}$$

Thus, $\bar{\mathbf{V}}^{\mathrm{energy}}$ is finally expressed as

$$\bar{V}_i^{\mathrm{energy}} = N_i \frac{v^{\mathrm{R}} v^{\mathrm{R}} + v^{\mathrm{I}} v^{\mathrm{I}}}{v^{\mathrm{R}}}. \tag{33}$$

By comparing equations 21 and 23 with 33, we conclude that $\bar{\mathbf{V}}^{\mathrm{energy}}$ for a stationary $\mathbf{p}$ yields exactly the same value as ray velocity V^{ray}. Hence, the main difference between the ray and energy velocities is that the energy velocity is defined for any complex-valued $\mathbf{p}$, but the ray velocity is defined just for stationary $\mathbf{p}$. For a stationary wave, both velocities have the same physical meaning.

Note that the stationary wave also displays other interesting properties. In anisotropic viscoelastic media, the instant energy flux of a time-harmonic plane wave has, in general, a time-dependent direction. For a stationary wave, the instant energy flux direction is constant.

NUMERICAL EXAMPLES

In this section, I demonstrate properties of ray velocity and ray attenuation on numerical examples performed for P-waves. I show the differences produced by different definitions of propagation velocities and attenuations. I adopted four transversely isotropic viscoelastic models with different strength of anisotropy and attenuation (see Tables 1 and 2). Their values are chosen to be close to observations for sedimentary rocks. The frequency of the signal is assumed to be 30 Hz.

The four models (A, B, C, and D) combine two models of velocity anisotropy and two levels of attenuation. The P-wave anisotropy is 23% for models A and B and 11% for models C and D (see Table 3). The level of attenuation for model A is twice as large as that for model B. The same applies to models C and D. The attenuation anisotropy is 68% for models A and B and 58% for models C and D. The Q-factor anisotropy is 48% for all four models.

Figure 1 shows the directional variations of phase and ray velocities, attenuations, and Q-factors for model A. The angles range from 0° to 90°. The velocities, attenuations, and Q-factors are calculated by using two approaches: (1) a correct method (described in the sections on Waves Generated by Point Sources and Calculation of Stationary Slowness Vector) based on evaluating velocities for stationary slowness vector $\mathbf{p}_0$ and (2) a simplified method based on evaluating velocities for a homogeneous slowness vector $\mathbf{p}$.

Figure 1 shows that the velocities calculated by using the two methods coincide, the differences between them being within the width of the line. The same result is obtained when attenuation is neglected. Hence, the attenuation in the models studied is not high enough to affect the velocities considerably. The errors in phase and ray velocities produced by using the simplified nonstationary method are about 0.05% or less (see Table 4). However, the errors in attenuations and Q-factors produced by the simplified method are more significant and clearly visible (see Figure 1c–f): 17.4% and 16.6% for the phase and ray attenuations and 28.3% and 30.9% for the phase and ray Q-factors, respectively (see Table 4). Such differences

Table 1. Viscoelastic parameters in the standard notation. The two-index Voigt notation is used for density-normalized elastic parameters a^{R}_{ijkl} and quality-factor matrix q_{ijkl}.

	Elastic parameters				Attenuation parameters			
Model	A^{R}_{11} (km^2/s^2)	A^{R}_{13} (km^2/s^2)	A^{R}_{33} (km^2/s^2)	A^{R}_{44} (km^2/s^2)	Q_{11}	Q_{13}	Q_{33}	Q_{44}
A	14.4	4.50	9.00	2.25	30	15	20	15
B	14.4	4.50	9.00	2.25	60	30	40	30
C	10.8	3.53	9.00	2.25	30	15	20	15
D	10.8	3.53	9.00	2.25	60	30	40	30

Table 2. Viscoelastic parameters in the Thomsen-style notation. For the definition of parameters in the Thomsen-style notation, see Thomsen (1986) and Zhu and Tsvankin (2006).

	Elastic parameters				Attenuation parameters			
Model	V_{P0} (km/s)	V_{S0} (km/s)	ε	δ	A_{P0} (10^{-2})	A_{S0} (10^{-2})	ε_Q	δ_Q
A	3.00	1.50	0.30	0.00	2.50	3.33	−0.333	0.667
B	3.00	1.50	0.30	0.00	1.25	1.67	−0.333	0.667
C	3.00	1.50	0.10	−0.10	2.50	3.33	−0.333	0.511
D	3.00	1.50	0.10	−0.10	1.25	1.67	−0.333	0.511

Table 3. P-wave velocity and attenuation anisotropy. $\bar{V}^{\mathrm{ray}}$, $\bar{A}^{\mathrm{ray}}$, and $\bar{Q}^{\mathrm{ray}}$ are the mean P-wave ray velocity, attenuation, and Q-factor; a_V^{ray}, a_A^{ray}, and a_Q^{ray} are the P-wave ray velocity anisotropy, attenuation anisotropy, and Q-factor anisotropy. The anisotropy is calculated as $a = 200(U_{\max} - U_{\min})/(U_{\max} + U_{\min})$, where $U_{\max}$ and $U_{\min}$ are the maximum and minimum values of the respective quantity.

Model	$\bar{V}^{\mathrm{ray}}$ (km/s)	a_V^{ray} (%)	$\bar{A}^{\mathrm{ray}}$ (s/km)	a_A^{ray} (%)	$\bar{Q}^{\mathrm{ray}}$	a_Q^{ray} (%)
A	3.28	23.3	75.2×10^{-4}	67.7	21.1	48.1
B	3.27	23.4	37.7×10^{-4}	67.8	42.2	48.1
C	3.06	10.5	78.8×10^{-4}	58.0	21.3	48.3
D	3.06	10.5	39.5×10^{-4}	58.0	42.6	48.3

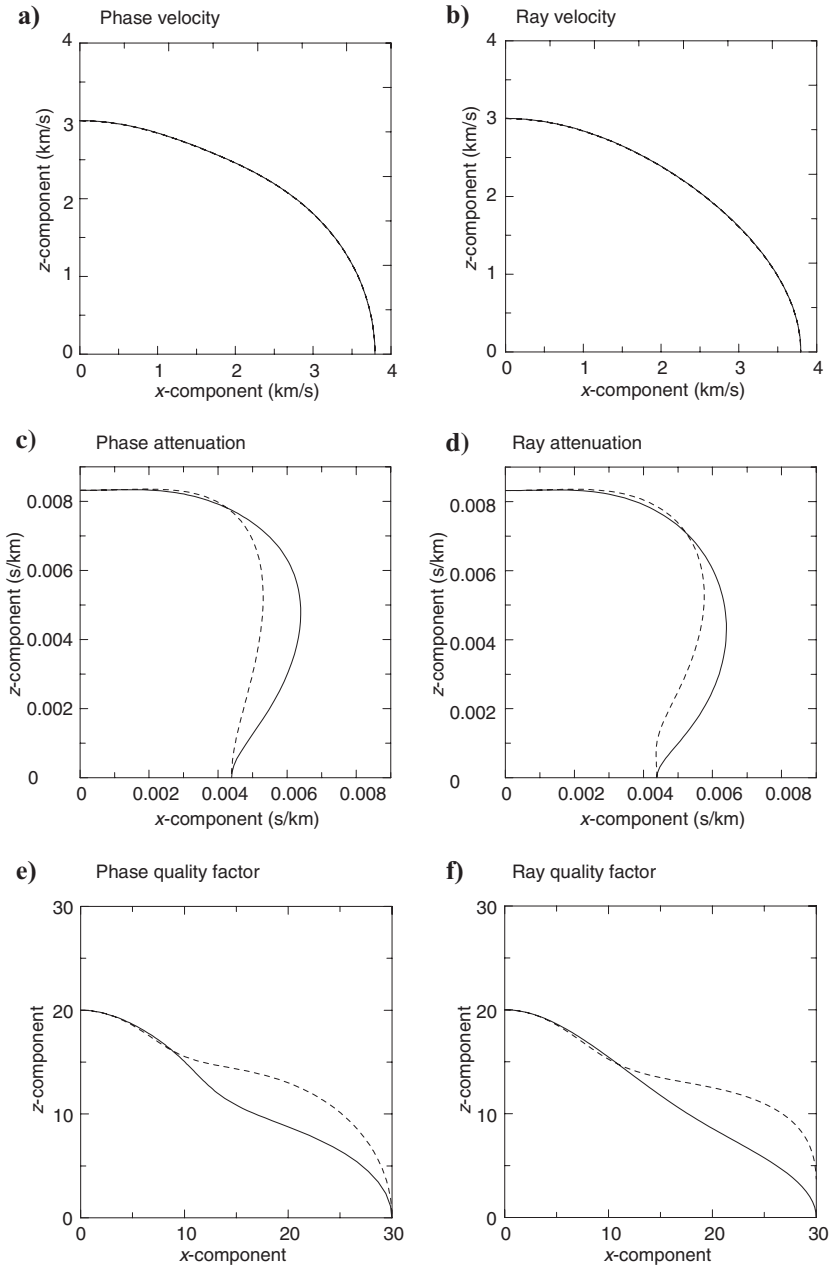

Figure 1. Polar plots of (a-b) the P-wave velocities, (c-d) attenuations, and (e-f) Q-factors in model A. Solid line — stationary approach (the slowness vector is inhomogeneous), dashed line — nonstationary approach (the slowness vector is homogeneous). For parameters of the model, see the text.

Table 4. Maximum errors of the nonstationary approach. The error for a particular ray is calculated as $E = 100|U^{\text{exact}} - U^{\text{approx}}|/U^{\text{exact}}$, where U^{exact} and U^{approx} are exact and approximate values of the respective quantity. The presented values are maxima over all rays.

Model	Error V^{phase} (%)	Error V^{ray} (%)	Error A^{phase} (%)	Error A^{ray} (%)	Error Q^{phase} (%)	Error Q^{ray} (%)
A	1.5×10^{-2}	5.3×10^{-2}	17.4	16.6	28.3	30.9
B	0.4×10^{-2}	1.4×10^{-2}	17.4	16.7	28.3	31.0
C	1.5×10^{-2}	4.5×10^{-2}	10.8	11.2	15.4	16.6
D	0.4×10^{-2}	1.1×10^{-2}	10.9	11.3	15.4	16.7

cannot be neglected; indeed, they point to the necessity of considering the proper stationary method in attenuation studies.

Figure 2 shows the velocities and attenuations for model C. Again, no visible differences are observed in velocities when applying the stationary and nonstationary methods. However, the differences in attenuations and Q-factors are significant: 10.8% and 11.2% for phase and ray attenuations and 15.4% and 16.6% for the phase and ray Q-factors, respectively.

The directional variations of velocities and attenuations for models B and D are almost identical to those for models A and C; therefore, I do not present them. The only difference between models A and B is that the attenuation and Q-factor plots for model B would be of a scale twice less than for model A. The scale of velocity plots and shape of velocity, attenuation, and Q-factor functions remains unchanged. The same applies to differences between models C and D.

Figure 3 shows the inhomogeneity of a stationary slowness vector as a function of a ray direction for models under study. The inhomogeneity projects into complex-valued slowness direction $\mathbf{n}$ parameterized by inclination angle θ and azimuth angle φ:

$$\mathbf{n} = \begin{bmatrix} \sin\theta\cos\varphi \\ \sin\theta\sin\varphi \\ \cos\theta \end{bmatrix}. \qquad (34)$$

Angle φ is always real valued because of symmetry of the medium. Angle θ is real valued for a simplified nonstationary approach but complex valued for a stationary approach. As seen from Figure 3, for the stationary approach, the imaginary part of θ is very small. Its absolute value is less than 1.2° for models A and C (more attenuative models) and even less than 0.6° for models B and D (less attenuative models). Hence, the imaginary part of angle θ decreases with decreasing attenuation. Nevertheless, even such tiny differences between the stationary and nonstationary slowness directions are visible at phase and ray attenuation plots (see Figures 1 and 2).

The differences between the stationary and nonstationary approaches also can be exemplified on wave amplitudes. Figure 4 shows the radiation pattern for an explosion buried in models A and B. The radiation pattern is plotted in the x-z-plane. The explosion is characterized by the moment tensor

$$M_{kl} = M_0 \begin{bmatrix} 1 & & \\ & 1 & \\ & & 1 \end{bmatrix}, \qquad (35)$$

where M_0 is the scalar moment. The amplitude R of the radiated wave is calculated for observation points at fixed distance from the explosion source by using the formula

$$R = \sqrt{u_i u_i^*}, \tag{36}$$

where

$$u_i = M_{kl} * \frac{\partial}{\partial x_l} G_{ik}^{\text{asym}}$$

and the symbol $*$ means the time convolution.

Figure 4 illustrates several interesting characteristics of radiated waves. First, it indicates that the radiation pattern of an explosion in an anisotropic medium can deviate significantly from a uniform, directionally independent radiation of an explosion in an isotropic medium (Figure 4a and c). Second, a nonuniform radiation is further pronounced with increasing distance owing to directionally dependent attenuation (Figure 4b and d). Under elastic anisotropy or anisotropy with isotropic attenuation, the radiation pattern can also be directionally dependent, but its shape cannot change with distance. On the contrary, a strong dependence of the radiation pattern on distance from the source is observed in Figure 4. Third, errors of wave amplitude calculated by using the nonstationary approach increase with distance. Obviously, the errors depend on the level of attenuation, being more pronounced for more attenuative models.

Note that plots for models C and D are not presented because they are similar to those in Figure 4.

DISCUSSION

The discrepancies in attenuation calculated for homogeneous and inhomogeneous waves are rather surprising and unexpected. So far, only a nonstationary approach has been applied and published in the literature (Carcione et al., 2003; Zhu and Tsvankin, 2006, 2007). This approach was expected to produce satisfactory results at least for low attenuation. Zhu and Tsvankin (2006, 2007), for example, argue that the inhomogeneity of a stationary slowness vector must be low for weakly attenuating media; therefore, the inhomogeneity effects must be of second order and thus negligible. However, the presented numerical examples indicate that the problem is more involved. Even though the inhomogeneity of a stationary slowness vector is low, it can produce significant effects in attenuation. The reason is that the inhomogeneity is controlled not only by attenuation but also by velocity anisotropy of the medium. Hence, the effects of the inhomogeneous slowness vector do not necessarily decrease with decreasing attenuation.

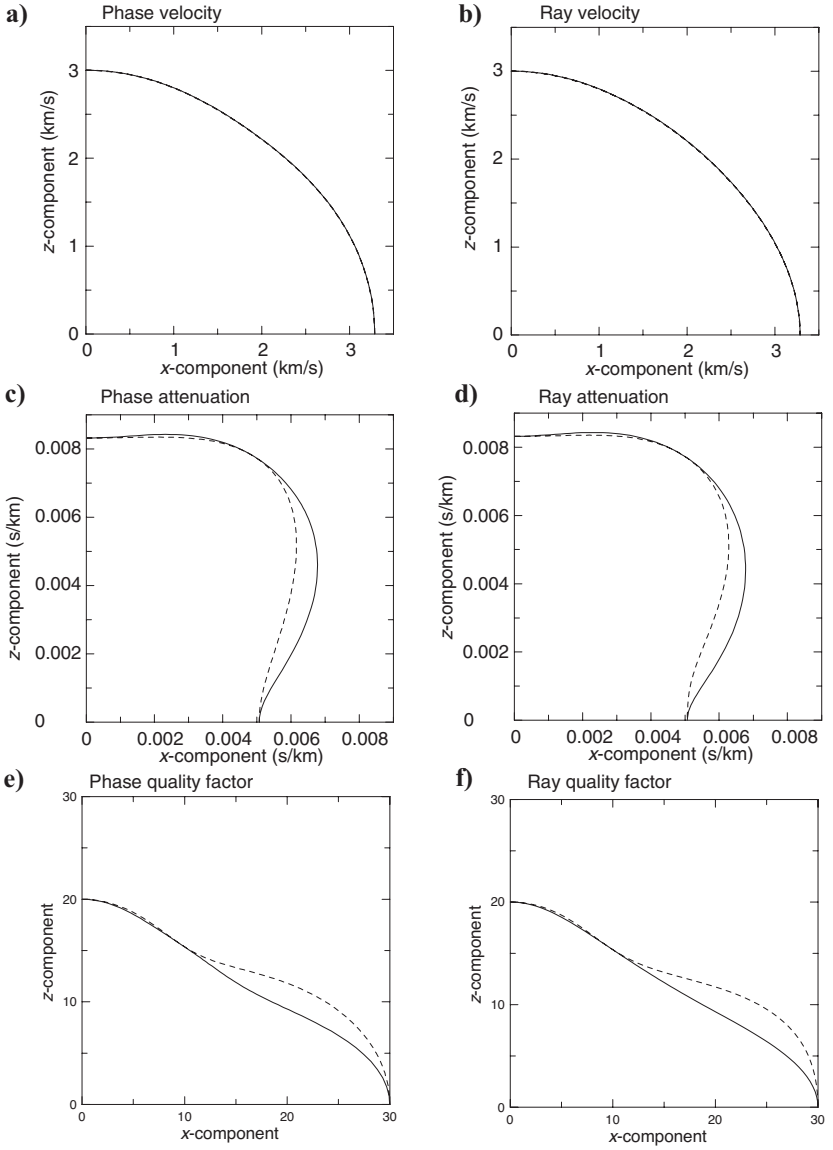

Figure 2. Polar plots of (a-b) the P-wave velocities, (c-d) attenuations, and (e-f) Q-factors in model C. For details, see the caption of Figure 1.

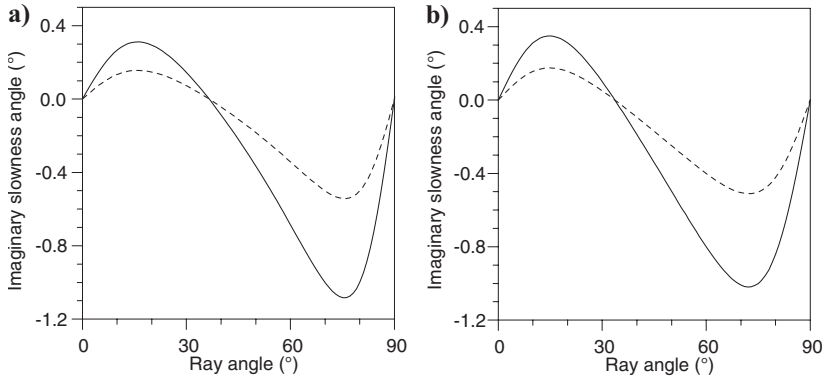

Figure 3. Imaginary part of the stationary slow+ness inclination angle as a function of the ray inclination angle. (a) Full line — model A; dashed line — model B. (b) Full line — model C; dashed line — model D. The imaginary part of the nonstationary slowness inclination angle is zero for all models.

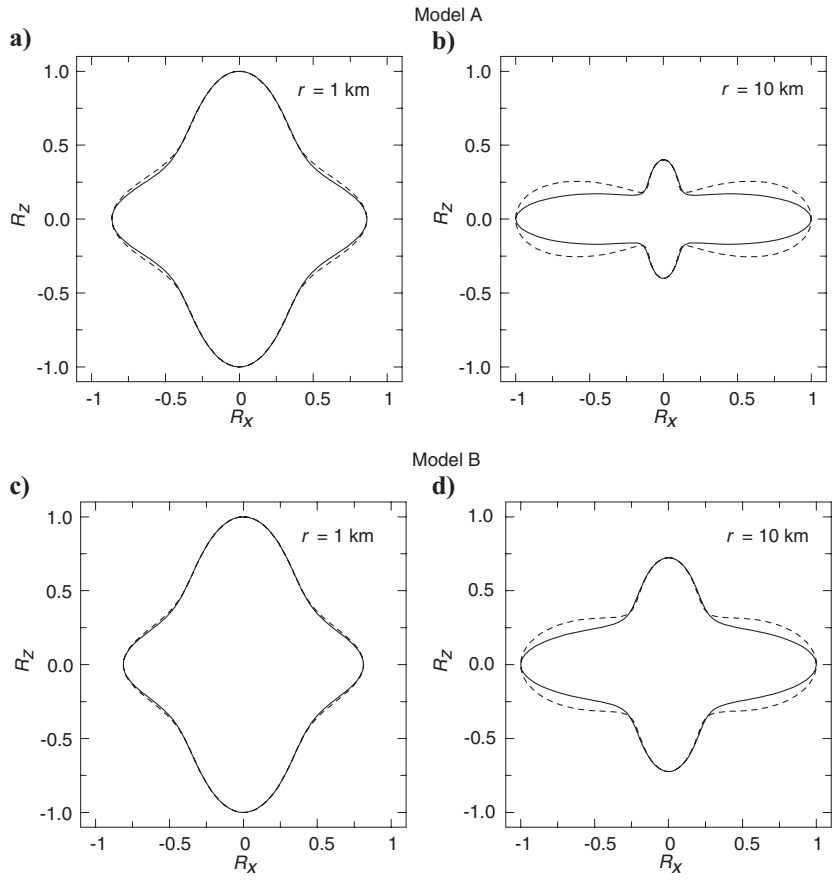

Figure 4. Radiation pattern of an explosion situated in (a-b) model A, and (c-d) model B. The wave amplitudes are calculated at two distances from the source: $r = 1$ km and $r = 10$ km. Full line — stationary approach; dashed line — nonstationary approach. The radiation patterns are plotted in the x-z-plane and normalized to their maximum amplitude.

CONCLUSIONS

Asymptotic wavefields in anisotropic viscoelastic media display some substantial differences compared with those in elastic media. Correct asymptotic wave quantities must be calculated by using a stationary slowness vector $\mathbf{p}_0$. This vector is defined as the slowness vector, for which the complex energy velocity is parallel to a ray. Because the ray direction is real, the complex energy velocity is homogeneous. Consequently, the stationary slowness vector $\mathbf{p}_0$ is, in general, inhomogeneous, and its computation involves finding two independent unit vectors that specify directions of its real and imaginary parts.

The stationary slowness vector can be calculated by using either an iterative inversion or a system of coupled polynomial equations of the sixth order. The iterative approach is safe and advantageous when anisotropy is free of triplications. In anisotropy with triplications, the latter approach is preferable. Once the stationary slowness vector is found, all asymptotic wave quantities such as polarization vectors, velocities, and amplitudes can readily be calculated. Subsequently, we can construct wavefronts and attenuation surfaces.

Numerical modeling indicates that asymptotic wave quantities have different sensitivities to the inhomogeneity of the stationary slowness vector $\mathbf{p}_0$. The most sensitive quantities are phase and ray attenuations and Q-factors. If attenuations and Q-factors are calculated approximately through the use of a homogeneous $\mathbf{p}$, the errors can attain values commensurate to the strength of velocity anisotropy. Hence, the errors can be as great as tens of percent for anisotropy observed in sedimentary rocks. This distortion applies to strongly as well as to weakly attenuative media.

ACKNOWLEDGMENTS

The author thanks T. Chichinina and three anonymous reviewers for their helpful reviews. The work was supported by the Grant Agency of the Czech Republic, grant 205/05/2182; by the Consortium Project, Seismic Waves in Complex 3D Structures, and by the EU Consortium Project Induced Microseismics Applications from Global Earthquake Studies (IMAGES), contract MTKI-CT-2004-517242. Part of the work was done while the author was a visiting researcher at Schlumberger Cambridge Research.

REFERENCES

Aki, K., and P. G. Richards, 2002, Quantitative seismology: University Science Books.

Audoin, B., and S. Guilbaud, 1998, Acoustic waves generated by a line source in a viscoelastic anisotropic medium: Applied Physics Letters, **72**, 774–776.

Auld, B. A., 1973, Acoustic fields and waves in solids: John Wiley & Sons, Inc.

Ben-Menahem, A., and S. J. Singh, 1981, Seismic waves and sources: Springer-Verlag.

Burridge, R., 1967, The singularity on the plane lids of the wave surface of elastic media with cubic symmetry: Quarterly Journal of Mechanics and Applied Mathematics, **20**, 41–56.

Carcione, J. M., 1990, Wave propagation in anisotropic linear viscoelastic media: Theory and simulated wavefields: Geophysical Journal International, **101**, 739–750. Erratum: 1992, 111, 191.

———, 1994, Wavefronts in dissipative anisotropic media: Geophysics, **59**, 644–657.

———, 2000, A model for seismic velocity and attenuation in petroleum source rocks: Geophysics, **65**, 1080–1092.

———, 2001, Wave fields in real media: Wave propagation in anisotropic, anelastic and porous media: Pergamon Press, Inc.

Carcione, J. M., and F. Cavallini, 1993, Energy balance and fundamental relations in anisotropic-viscoelastic media: Wave Motion, **18**, 11–20.

Carcione, J. M., K. Helbig, and H. B. Helle, 2003, Effects of pressure and saturating fluid on wave velocity and attenuation in anisotropic rocks: International Journal of Rock Mechanics and Mining Sciences, **40**, 389–403.

Carcione, J. M., D. Kosloff, and R. Kosloff, 1988, Wave propagation simulation in anisotropic (transversely isotropic) medium: Quarterly Journal of Mechanics and Applied Mathematics, **41**, 320–345.

Carcione, J. M., G. Quiroga-Goode, and F. Cavallini, 1996, Wavefronts in dissipative anisotropic media: Comparison of the plane wave theory with numerical modeling: Geophysics, **61**, 857–861.

Červený, V., and I. Pšenčík, 2005, Plane waves in viscoelastic anisotropic media — I. Theory: Geophysical Journal International, **161**, 197–212; http://dx.doi.org/10.1111/j.1365-246X.2005.02589.x.

———, 2006, Energy flux in viscoelastic anisotropic media: Geophysical Journal International, **166**, 1299–1317; http://dx.doi.org/10.1111/j.1365-246X.2006.03057.x.

Chichinina, T., V. Sabinin, and G. Ronquillo-Jarillo, 2006, QVOA analysis: P-wave attenuation anisotropy for fracture characterization: Geophysics, **71**, no. 3, C37–C48; http://dx.doi.org/10.1190/1.2194531.

Deschamps, M., and F. Assouline, 2000, Attenuation along the Poynting vector direction of inhomogeneous plane waves in absorbing and anisotropic solids: Acustica, **86**, 295–302.

Deschamps, M., B. Poirée, and O. Poncelet, 1997, Energy velocity of complex harmonic plane waves in viscous fluids: Wave Motion, **25**, 51–60.

Every, A. G., and K. Y. Kim, 1994, Time domain dynamic response functions of elastically anisotropic solids: Journal of the Acoustical Society of America, **95**, 2505–2516.

Moczo, P., J. O. A. Robertsson, and L. Eisner, 2007, The finite-difference time-domain method for modelling of seismic wave propagation, *in* R.-S. Wu and V. Maupin, eds., Advances in wave propagation in heterogeneous earth: Elsevier-Academic Press, 421–516; http://dx.doi.org/10.1016/S0065-2687(06)48008-0.

Press, W. H., S. A. Teukolsky, W. T. Vetterling, and B. P. Flannery, 2002, Numerical recipes: The art of scientific computing: Cambridge University Press.

Saenger, E. H., and T. Bohlen, 2004, Finite-difference modeling of viscoelastic and anisotropic wave propagation using the rotated staggered grid: Geophysics, **69**, 583–591; http://dx.doi.org/10.1190/1.1707078.

Shuvalov, A. L., and N. H. Scott, 1999, On the properties of homogeneous viscoelastic waves: Quarterly Journal of Mechanics and Applied Mathematics, **52**, 405–417.

Thomsen, L., 1986, Weak elastic anisotropy: Geophysics, **51**, 1954–1966.

Vavryčuk, V., 1999, Properties of S waves near a kiss singularity: A comparison of exact and ray solutions: Geophysical Journal International, **138**, 581–589; http://dx.doi.org/10.1046/j.1365-246X.1999.00887.x.

———, 2002, Asymptotic elastodynamic Green function in the kiss singularity in homogeneous anisotropic solids: Studia Geophysica et Geodaetica, **46**, 249–266; http://dx.doi.org/10.1023/A:1019854020095.

———, 2006, Calculation of the slowness vector from the ray vector in anisotropic media: Proceedings of the Royal Society, Series A, **462**, 883–896; http://dx.doi.org/10.1098/rspa.2005.1605.

———, 2007, Asymptotic Green function in homogeneous anisotropic viscoelastic media: Proceedings of the Royal Society, Series A, 463, 2689–2707; http://dx.doi.org/10.1098/rspa.2007.1862.

Yeatts, F. R., 1984, Elastic radiation from a point source in an anisotropic medium: Physical Review B, **29**, 1674–1684.

Zhu, Y., and I. Tsvankin, 2006, Plane-wave propagation in attenuative transversely isotropic media: Geophysics, **71**, no. 2, T17–T30; http://dx.doi.org/10.1190/1.2187792.

———, 2007, Plane-wave attenuation anisotropy in orthorhombic media: Geophysics, **72**, no. 1, D9–D19; http://dx.doi.org/10.1190/1.2387137.